Indian Journal of Chemistry
Vol. 62, March 2023, pp. 217-229
DOI: 10.56042/ijc.v62i3.71998

Interaction of dpyatriz and Cu/Zn-dpyatriz complexes with human telomere DNA: The role of G-quadruplex formation and its effect on antitumor and antitelomerase activity

Duraisamy Renuga[a], Palanisamy Uma Maheswari [b,]* & K.M. Meera Sheriffa Begum[b]

[a]Department of Chemistry, Selvamm Arts and Science College, Namakkal 637 003, Tamilnadu, India
[b]Department of Chemical Engineering, National Institute of Technology, Tiruchirappalli 620 015, India

*E-mail: pumatry74@gmail.com

Received 13 September 2021; accepted (revised) 23 December 2022

1,3,5-Triazine derivative of dipyridyl amine (dpyatriz) and the Cu(II), Zn(II) complexes have been prepared, characterized by CHN, IR, NMR and mass measurements and interacted with $HTelo_8$ and $HTelo_{20}$, the two types of human telomere repeat DNA (TTAGGG)n; n = 8, 20. The telomere DNAs have been treated with all three compounds (dpyatriz, Cu-dpyatriz and Zn-dpyatriz) under parallel/antiparallel and random coiled conditions. The interactions are followed by circular dichrosim measurements, fluorescent intercalator displacement (FID) assays and molecular docking studies through MOE program. The free ligand and its Cu(II) and Zn(II) complexes stabilize predominantly antiparallel G-quadruplex form under antiparallel and no salt conditions. The binding constant (K_b) values calculated for the ligand and complexes are in the range of 1.9 x 10^5 M^{-1} to 4.2 x 10^7 M^{-1} under various conditions show the higher affinity of G-quadruplex conformations. The FID assay using thiazole orange with $HTelo_{20}$ clearly depicts the G-quadruplex stabilization through strong binding mode. Also, all the three compounds dpyatriz, Cu-dpyatriz and Zn-dpyatriz show an intercalative mode of interaction with antiparallel G quadruplex DNA in molecular docking studies. The compounds show cytotoxicity with the IC_{50} values in the range of 50 – 90 nM, and antitelomerase activity in the range of 5 to 10 μM.

Keywords: G-quadruplex, Triazine, Dipyridyl amine, Antitelomerase, Anticancer, Human telomere

The telomerase enzyme which is responsible for the maintenance of telomere length in cancer cells and thus for their immortalisation, catalyses the formation of telomeric DNA repeats[1]. Telomerase, is also considered as a biomarker for finding the stage of cancer as it is expressed in 80–90% of cancer cells, but not in normal somatic cells[2,3]. So, it is therefore considered as molecular target for selective therapeutic intervention. The human telomere DNA with its TTAGGG repeat sequence tend to form inter/intramolecular G-quadruplex secondary conformation in the presence of suitable small-molecules[4–7] (Scheme 1).

The stacked conformation of guanines together in quadruplex formation may physically detach the association of telomere substrate to the active part of the telomerase enzyme and other telomere-binding proteins, which would turn on a DNA damage signal and eventual inducement of apoptosis pathways[8]. A large number of such quadruplex-binding/inducing/ stabilizing molecules have been studied, and most of them possess a planar aromatic chromophore such as an acridine, anthraquinone, perylene diimides and porphyrin derivatives[9–15] which can interact with the planar G-quartet surface of a quadruplex through π-π interactions. Also the substituents containing hetero aromatic chromophores like the natural product telomestatin, neomycin conjugates, pyridine, phenanthroimidazole and triazine derivatives also tend to stabilize G-quadruplexes[16–20]. The binding affinity of these ligands can further improved by the presence of positive charge. 1, 3, 5-Triazine derivatives are widely used as herbicides, drugs or polymers like melamine formaldehyde that has excellent thermal and electrical properties. They have exhibited promising potential as antitumor agents, enzyme inhibitors, and other bioactive agents. However, their metal complexes received little attention for biological applications partly due to their poor solubility in both water and common organic solvents. The dipyridyl amine based Ru, Rh and Ir complexes were reported in the synthesis of luminescent compounds and nickel complexes were used in the copper-catalyzed oxidation of DTBC had

the activity of the catalyst[21–25]. Also the Ir(III) complexes had the stronger influence in photophysical properties and Fe(II) complexes are used in the formation of insoluble molecular material consisting of 1D polymeric chains and showing great diversity in magnetic behavior[26–29]. Number of pseudo polymorphic phases was derived from Pt(II) complex of this ligand and used in the development of new antitumor agents dpyatriz acts as an hexadentate ligand with Zn(II) and Co(II) complexes. Some of the Zn(II) complexes have been found to be efficient fluorescent sensors for benzene molecules,

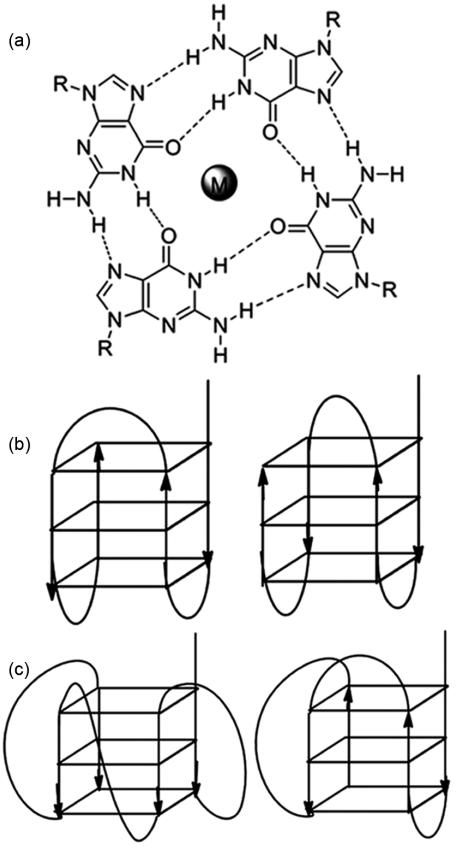

Scheme 1 — (a) G-tetrad, (b) parallel and (c) antiparallel G-quadruplexes

photoluminescent properties of this ligand derivatives were also investigated for their electroluminescent applications, Copper complexes are extensively studied and accepted because of their biologically accessible redox potential values[30–33]. Trinuclear complexes of Cu(II) used as building blocks for the controlled assembly of 2D honeycomb-type networks and shows prominent DNA cleavage activity[34,35]. Fluorescent titration experiments of Cu(I) and Ag(I) complexes of this ligand has distinct electronic property differences. This ligand and its Pd(II) complex have been of particular interest for use in organic light emitting diodes (OLEDs) largely due to their good film forming properties[36,37]. Although, numerous reports of this star shaped ligand and their metal complexes were available and extensively used in earlier literature for their magnetic and photophysical properties, but their biological activity applications have not been explored so far, only few of them are reported. Accordingly, in this paper we discuss the results on interaction of 1,3,5-triazine derivative of dipyridylamine and its Cu(II), Zn(II) complexes (Fig. 1) with telomere DNA to stabilize G-quadruplex conformation and their application towards antitelomerase and anticancer properties.

Experimental Details

Materials and Methods

Cyanuric Chloride, DIPEA, 2,2'-dipyridylamine, THF, $CDCl_3$, Ethanol, Methanol, $CuCl_2$, $ZnCl_2$ were purchased from sigma-aldrich and of analytical grade. Calf thymus DNA (CT DNA) and Human telomeric DNA with short and long range ($HTelo_8$ and $HTelo_{20}$) were purchased from Microsynth, Swizterland. For the biological studies milli Q water was used. The distilled and dried organic solvents were used for the synthesis. The stock of the compounds synthesized were prepared in DMSO for biological studies, and then appropriately diluted with phosphate buffer. The FT-IR spectrum was recorded in Alpha Bruker

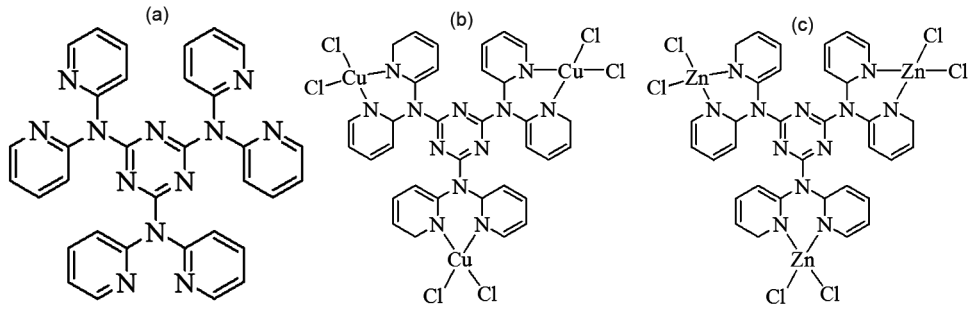

Fig. 1 — (a) Ligand dpyatriz, (b) Cu-dpyatriz and (c) Zn-dpyatriz compounds

spectrophotometer. CHN analysis was done on a Perkin-Elmer 2400 series II analyser. ^{1}H and ^{13}C NMR were done on Bruker 500 MHz.

Preparation of dpyatriz

Cyanuric chloride (5 mmol) was dissolved in THF and refluxed for 10 min. Then the base diethylisopropylamine (DIPEA) was dissolved in 5 mL of THF and was added dropwise to the reaction mixture and refluxed for another 10 min. To this mixture, 15 mmol of 2,2'-dipyridylamine was added under stirring condition. Then the total mixture was refluxed continuously for another 48 h. The solvent of the reaction mixture was removed under pressure and the product was isolated as pale white solid. To this solid excess double distilled water was added and stirred for 24 h to remove HCl salt, then the precipitate was filtered and weighed 2.061 mg [38]. The synthesis scheme is shown in Scheme 2.

Synthesis of the complexes

The Cu(II) and Zn(II) complexes of dpyatriz ligand were prepared by reacting the ligand in methanol to $CuCl_2$ or $ZnCl_2$ solution in methanol at 1: 3; ligand to metal ratio, respectively. The resulting mixtures were stirred at 60°C for 6 h, and then it was cooled to room temperature. Green precipitate was obtained for Cu-dpyatriz and pale white color precipitate was obtained for Zn-dpyatriz after filtering[39]. The complexes were dried under vacuum in the oven. The yield was calculated as 65% (3.22 mg) for Cu-dpyatriz and 72% (3.59 mg) for Zn-dpyatriz. The synthesis scheme is shown in Scheme 3. The CHN analysis report and observed spectra for all the compounds are shown in Table S1 and Fig. S1-S6, respectively, in Supplementary Information.

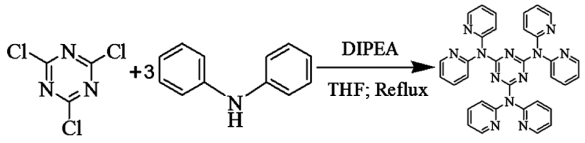

Scheme 2 — Synthesis of the ligand dpyatriz

Characterizations of Cu-dpyatriz

MALDI-TOF m/z: 991.98 $[Cu_3C_{33}H_{24}N_{12}Cl_6]^+$. Elemental analysis calculated (%) for $C_{33}H_{24}N_{12}Cl_6Cu_3$: C, 39.96; H, 2.44; N, 16.94; % found: C, 39.13; H, 2.48; N, 16.12; IR (KBr): 3147 (m), 1603 (s), 1551 (s), 1466 (s), 1381 (s), 1299 (s), 1157 (s), 774 (m), 651 (m) cm^{-1}.

Characterizations of Zn-dpyatriz

MALDI-TOF m/z: 994.52 $[Zn_3C_{33}H_{24}N_{12}Cl_5+CH_3OH]^+$. Elemental analysis calculated (%) for $C_{33}H_{24}N_{12}Cl_6Zn_3$: C, 39.73; H, 2.42; N, 16.85; % found: C, 39.12; H, 2.46; N, 16.11. IR (KBr):3147 (m), 1604 (s), 1552 (s), 1466 (s), 1377 (s), 1299 (s), 1155 (s), 771 (m), 651 (m) cm^{-1}.

Circular dichroic spectral studies

Circular dichroic (CD) spectra of calf thymus DNA (CT DNA), $HTelo_8$ and $HTelo_{20}$ of human telomeric DNA sequence in different buffers with or without compounds treated were recorded by using JASCO J-715 spectropolarimeter at 37°C. All experiments were done using 0.2 cm path quartz cell. Each CD spectrum was collected after averaging over at least 5 accumulations using a scan speed of 100 nm min^{-1} and 1 s response time. Machine plus cuvette baselines were subtracted and the resultant spectra zeroed outside the absorption bands. Necessary equilibration time (normally 5 min) was allowed prior to the collection of each spectrum. CD-melting studies of $d(TTAGGG)_n$ 10 x 10^{-5} M incubated under no salt conditions with the compounds dpyatriz, Cu-dpyatriz and Zn-dpyatriz were performed by measuring OD at 290 nm. Absorption spectra from 200 to 350 nm was collected as a function of temperature at a ramping rate of 1 °C/min. UV measurements were performed on a Cary 60 UV–visible spectrometer (Agilent, USA). Melting temperature (Tm) of each sample was obtained by first derivative analysis of obtained denaturation curves using of Origin 9.0. CD data are commonly reported as ellipticity (θ), which is related to absorbance by a factor of 32.98 ($\theta = 32.98\ \Delta_{Abs}$).

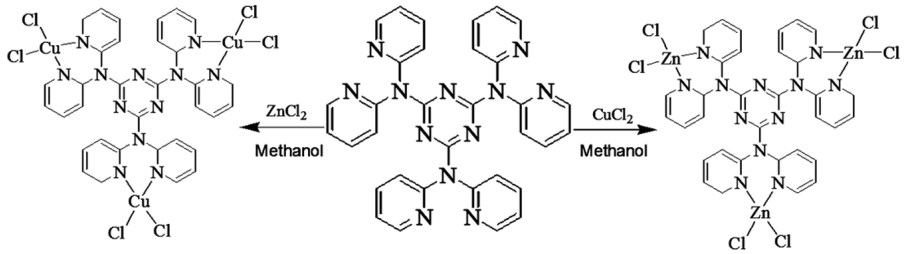

Scheme 3 — Synthesis of the complexes Cu-dpyatriz and Zn-dpyatriz

Conversion from molar extinction (absorbance corrected for concentration) to molar ellipticity uses a factor of 3298 ([θ] = 3298Δε). By using these equations above absorbance was calculated and applied. With the purpose to quantitatively compare the binding strength, the intrinsic binding constant (K_b) values of the complexes with Human telomere DNA were calculated by the following equation,[40].

$$\frac{[DNA]}{\varepsilon_a - \varepsilon_f} = \frac{[DNA]}{\varepsilon_b - \varepsilon_f} + \frac{1}{K_b (\varepsilon_b - \varepsilon_f)}$$

Where ε_a, ε_f, and ε_b are the apparent, free and bound complex extinction coefficients, respectively. A plot of [DNA]/($\varepsilon_a - \varepsilon_f$) versus [DNA] gave a slope of 1/($\varepsilon_b - \varepsilon_f$) and a Y intercept equal to $1/K_b(\varepsilon_b - \varepsilon f)$; K_b is the ratio of the slope to the Y intercept.

Fluorescent intercalator displacement assay

FID assay is used to check the ability of the treating compounds to displace thiazole orange (TO), the specific G-quadruplex intercalator bound to the nucleic acid, upon their strong binding. The fluorescence spectra of TO bind to the nucleic acid were recorded with λ_{ex} at 491 nm and λ_{em} at 580 nm. The experiments were done in JASCO spectrofluorimeter with base line corrected using appropriate reference cell at 25°C. The cuvettes are of 1 cm path length and made out of quartz. The DNA sample of d(TTAGGG) concentrations used were 5 x 10^{-6} M (in 10 mM phosphate buffer) and the $HTelo_{20}$ were stabilized under appropriate parallel or antiparallel conditions as required. The TO concentration used was 10 x 10^{-6} M and the compounds concentration used was 15 x 10^{-6} M. An incubation time of five minutes was given before each spectrum recording for equilibration.

Molecular docking and dynamics

Molecular docking studies were carried out using Molecular Operating Environment (MOE v.2019.01) software package (Chemical Computing Group, Montreal, Canada) to investigate the binding mode and interactions between the synthesized compounds and the receptor telomeric DNA. The pure ligand dpyatriz and their Cu-dpyatriz, Zn-dpyatriz complexes were built using chemdraw office ultra (R) version 7.0.4. These structures were converted into three-dimensional coordinates of MOE files and energy minimized. The MDB format of the ligand and complexes were obtained using MOE v.2019.01 software with potential fixed and partial charges added. These compounds were docked with X-ray or NMR derived telomere DNA stabilized in parallel (PDB ID: 1KF1), antiparallel (PDB ID: 2MCO) and hybrid (PDB ID: 6CCW) conformations. These PDB files of telomere DNA were converted to .MOE files, H_2O added and energy minimized. The RMS gradient was fixed as 0.1 kcal/mol/Å. Atoms farther than 8Å were fixed. Docking of the receptor DNA with the above mentioned compounds were done using the method triangle matcher and with scoring function London dG in GBV/WSA dG force fields. The refinement of the docking data was done under induced fit protocol. The output was based on 30 runs and the best five poses with the lowest RMSD were shown, and the one selected as the best binding mode was based on again the least RMSD value. Further interaction map and binding energies were obtained as the induced fit docking results.

Antitelomerase assay

The TRAP assay was done by using TRAPeze kit from Sigma-Aldrich. The concentrations of the compounds used were from 1 µM to 250 µM, and even from the lowest concentrations, PCR amplification products could not be observed, except for the control, 36 bp amplification product. The non-radiative polyacrylamide gel was used to view the products.

Anticancer studies

The MTT assay measures the cell proliferation rate or the cell viability based on the cell metabolic activity. The adenoma stage respective cancer cell lines, which are kept under constant cultures were treated with the compounds and were analysed for cytotoxicity profile using the MTT assay as described by Alley *et al.*[42]. The method uses (2-(4,5-dimethylthiazol-2-yl)- 2,5-diphenyl-2Htetrazolium bromide), for the mitochondrial reduction in living cells to produce blue insoluble purple formazan crystals. The cells used for the study were cultured in McCoy's medium, with 10% fetal calf serum and the antibiotics streptomycin (100 µg/mL) penicillin (100 units/mL). For the assay, cells were placed in 96 well plates and cultured in the above-said buffer for 24 h under 5% CO_2 atmosphere at 37°C. Then the compounds were added to the micro well plates, appropriately from the stock (in DMSO) to the final concentrations of 0-200 µM. An incubation period of 48 h was allowed and the cell survival conditions were determined by the absorbance of DMSO dissolved formazan crystals at 590 nm. This was done

using a BIO-RAD microplate reader (model 680). The concentration of the complex that kills the cell growth to 50% in comparison to the starting control was calculated from the graph obtained by plotting the cell survived (%) and the complex concentration (in μM). The results reported are an average of three experiments. The Graph Pad Prism Software, version 3.0, 2000 was used to construct the graph and analyse the data.

Results and Discussion

Synthesis and characterization

The ligand dpyatriz was prepared by a simple condensation method as explained[38] in the experimental section. The yield obtained was 70%. ESI-MS m/z: 589 $[M+H]^+$. Elemental analysis calculated (%) for $C_{33}H_{24}N_{12}$: C, 67.33; H, 4.10; N, 28.55; % found: C, 67.16; H, 4.48; N, 28.74. IR (KBr): 3147 (m), 1567 (s), 1488 (s), 1408 (s), 1352 (s), 1234 (s), 1168 (s), 1082 (m), 860 (m), 802 (s), 755 (s). ^{1}H NMR ($CDCl_3$, 500 MHz) 6.90 (d, 6H, py-H), 7.33 (m, 6H, py-H), 7.66 (m, 6H, py-H), 8.51 (d, 6H, py-H) ppm; ^{13}C NMR ($CDCl_3$, 500 MHz) 121.1(6C, py-C), 122.9(6C, py-C), 137.4(6C, py-C), 145.2(6C, py-C), 157.9(6C, py-C), 164.4(3C, triazine-C) ppm. Mass data of dpyatriz, Cu-dpyatriz and Zn-dpyatriz complexes are shown in Table 1.

Circular dichrosim (CD) studies

The compounds dpyatriz, Cu-dpyatriz and Zn-dpyatriz were interacted with two different human telomere DNA sequence, $HTelo_8$ and $HTelo_{20}$. $HTelo_8$ – a DNA sequence of $d(TTAGGG)_8$ with a repeat of eight (in total 40 bases) and $HTelo_{20}$ - a DNA sequence of $d(TTAGGG)_{20}$ with a repeat of twenty (in total 140 bases) are used to study the interactions of the compounds under study towards G-quartet formation and G-quadruplex stabilization. $HTelo_8$ has the ability to form G-quadruplex at short-range and $HTelo_{20}$ expected to form 4 to 6 G-quadruplex structures in long range. The selection of two different HTelo DNA in short and long range order are to check the ability of the compounds to stabilize the G-quartet and then to G-quadruplexes under parallel and antiparallel stabilized conditions (100 mM KCl and 100 mM NaCl, respectively) and also with no cationic conditions which is a random coiling form. The parallel or antiparallel G-quadruplex conformation adapted by the human telomeric DNA sequence d(TTAGGG)n under induced conditions shall be effectively described by circular dichroic spectral features. The base lines for buffer and the compound absorptions were appropriately deducted in the telomere DNA response during the compounds titration. The compounds were added incrementally with increasing concentration in 1:5 ratio (DNA:compound) and the interactions were followed by circular dichroism spectroscopy. The parallel G-quadruplex conformation stabilized under 10 mM phosphate buffer, 100 mM KCl shows a negative band around 240 nm because of right-handed helicity and a positive band around 275 nm due to base-stacking[42]. The antiparallel G-quadruplex conformation stabilized under 10 mM Phosphate buffer, 100 mM NaCl shows a positive band at 240 nm and negative band at 260 nm together a base stacking band at 290 nm[43].

When $HTelo_8$ stabilised under parallel G-quadruplex conditions was treated with the pure ligand and Zn-dpyatriz, the negative 240 nm elipticity band was stabilized and due to base stacking band at 290 nm depicting the G-quartet formation (Fig. 2). In $HTelo_{20}$, under parallel G-quadruplex condition, the pure ligand, and Zn-dpyatriz were found to interacted in such a way that the negative band at 240nm decreases along with the 290nm band increase similar to the $HTelo_8$ DNA (Fig. 2). This effect was observed previously by many literature reports[44–46]. In conclusion $HTelo_8$ and $HTelo_{20}$, under parallel G-quadruplex condition, the ligand dpyatriz and Zn-dpyatriz stabilized the induced antiparallel conformation. But the Cu-dpyatriz showed the intensity increase at 290 nm base stacking band with $HTelo_8$ and $HTelo_{20}$ and the negative helicity band at 240 nm began to increase with $HTelo_{20}$. Thus interaction of Cu-dpyatriz with $HTelo_{20}$ DNA clearly stabilized antiparallel G-quadruplex conformation with some induced CD intensity due to Cu-dpyatriz stacking over bound Cu-complexes[47,48]. Because of the presence of external loop residues all CD spectra

Table 1 — Mass data of dpyatriz, Cu-dpyatriz and Zn-dpyatriz complexes

Compound	Molecular formula	Molecular weight calculated	Molecular weight observed
dpyatriz	$C_{33}H_{24}N_{12}$	588.58	589 $[C_{33}H_{24}N_{12} + H]^+$
Cu-dpyatriz	$Cu_3C_{33}H_{24}N_{12}Cl_6$	991.98	991.98
Zn-dpyatriz	$Zn_3C_{33}H_{24}N_{12}Cl_6$	997.51	997.52

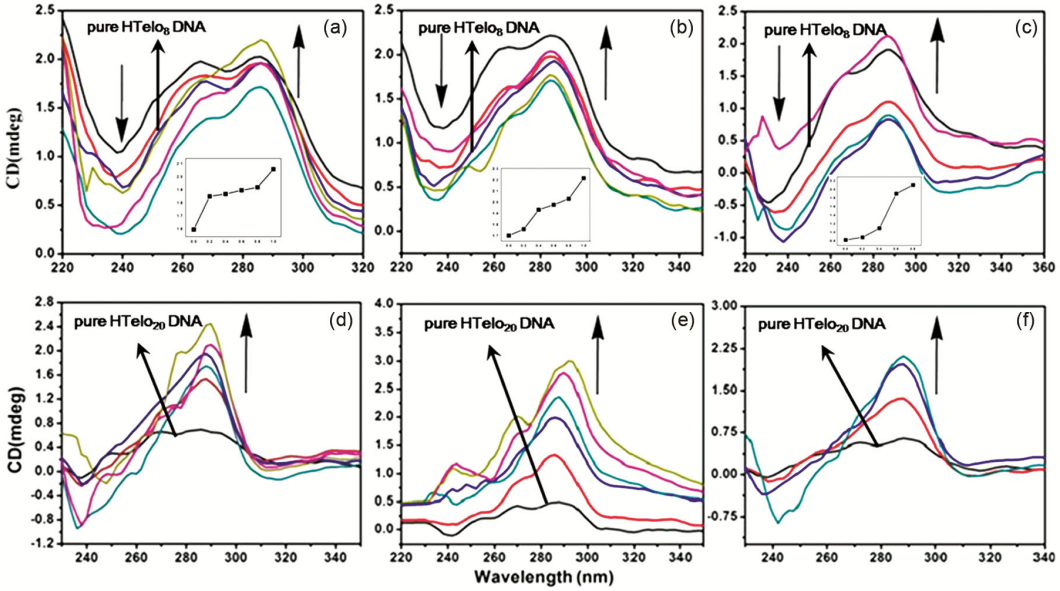

Fig. 2 — CD spectra of $HTelo_8$ under parallel G-quadruplex stabilized conditions (10×10^{-6}M) treated upto 5 equivalents of (a) dpyatriz, (b) Cu-dpyatriz and (c) Zn-dpyatriz; CD spectra of $HTelo_{20}$ under parallel G-quadruplex stabilized conditions (9.9×10^{-5}M) treated upto 5 equivalents of (d) dpyatriz, (e) Cu-dpyatriz and (f) Zn-dpyatriz

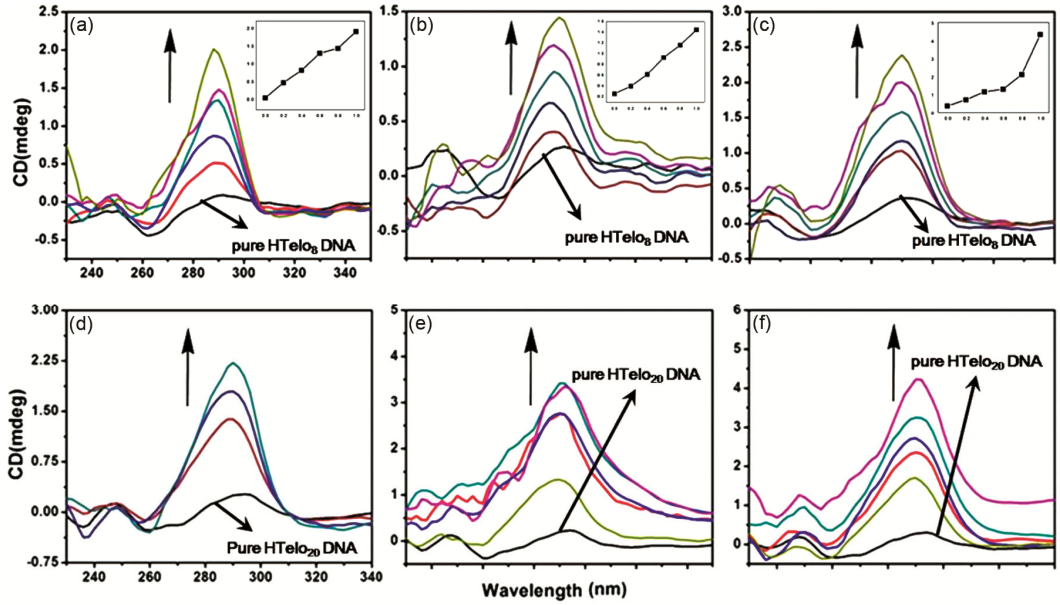

Fig. 3 — CD spectra of $HTelo_8$ under antiparallel conditions (7.14×10^{-5}M) treated upto 5 equivalents of (a) dpyatriz, (b) Cu-dpyatriz and (c) Zn-dpyatriz; CD spectra of $HTelo_{20}$ under parallel G-quadruplex stabilized conditions (9.28×10^{-5}M) treated upto 5 equivalents of (d) dpyatriz, (e) Cu-dpyatriz and (f) Zn-dpyatriz

under parallel conditions shown a dominant band at 290 nm which revealed the coexistence of dimeric parallel G-quadruplex structures[49–51]. It has been resulted that the interaction of compounds with $HTelo_8$ and $HTelo_{20}$ under the solution of K^+ forms a chair-type quadruplex, as a replacement to the basket-type structure[52–54].

$HTelo_8$, when stabilized under antiparallel G-quadruplex conditions with the pure ligand dpyatriz, Cu-dpyatriz and Zn-dpyatriz, the negative band at 260 nm was not disturbed by all the compounds and the positive bands at 242 and 290 nm were highly stabilized with the increase in the intensity revealed the stability of antiparallel G-quadruplex conformation as a yield of the interactions with compounds treated[55] (Fig. 3). On interaction with $HTelo_{20}$ under antiparallel conditions, very similar observations as for $Htelo_8$ were found on

interaction with all the three compounds and confirmed the antiparallel stabilization both in the short and long range sequences (Fig. 3).

When $HTelo_8$ and $HTelo_{20}$ under no salt conditions were treated with dpyatriz, Cu-dpyatriz and Zn-dpyatriz the antiparallel G-quadruplex conformation was stabilized with a lot increase in the CD intensity at 290 nm band[45,56]. Also the band at 260 nm showed increase on incremental addition of all the three compounds (Fig. S7). Inspite of the fact, without any prior incubation step of DNA and the compounds, the conformations got stabilized within five minutes for parallel and antiparallel G-quadruplex conformations under K^+, Na^+ and no salt conditions, respectively. On the whole, these results suggested that all compounds selectively induce or stabilize the antiparallel quadruplex form of telomeric DNA under the presence of K^+ or Na^+ ions and no salt solutions.

The parallel or antiparallel G-quadruplex stabilization may be due to the presence of strong π-π interaction between the triazine, pyridine ring of the ligand and guanine bases of the DNA, the stabilization of G-quadruplexes under no salt conditions depicts the ability of the ligand and its complexes towards orienting the guanines toward G-quartet formation and coupling the G-quartet towards G-quadruplexes. Hence the compounds dpyatriz, Cu-dpyatriz and Zn-dpyatriz have high affinity to induce and stabilize parallel and antiparallel G-quadruplexes. The changes seem to be irreversible, which are tested through ethidium bromide treatment, a classical intercalator which would revert any molecular binding by its classical intercalation binding mode (data not shown). Additionally, based on the intensity values obtained in the titration, the ligand or complex-DNA binding constant, K_b, was calculated as described in the experimental procedure.

The K_b values reported in the literature for the complexes like salicylidene-phenyldiamine complexes of Ni(II) and Cu(II) were 5.42×10^6 M^{-1} and 1.42×10^6 M^{-1}[Ref.57] and for the schiff-base complexes of Cu(II) and Zn(II) were 2.04×10^5 M^{-1} and 1.98×10^5 M^{-1}[Ref.58], under parallel conditions. Copper or magnesium – carrole complexes are reported with the binding constants values as 2.16×10^4 and 4.34×10^3 M^{-1}[Ref.59] and for trinuclear Ru(II) polypyridyl complex it was reported as 2.44×10^5 M^{-1}[Ref.60] under antiparallel conditions. Our compounds binding constants are in the order of 1.9×10^5 M^{-1} to 4.2×10^7 M^{-1} (Table 2) under parallel, antiparallel and no salt G-quadruplex conditions. These K_b values strongly suggest the high affinity binding of the compound to telomere DNA and their folding to G-quadruplex conformations.

Irrespective of the cation present (K^+ or Na^+) or without any cations our compounds were able to stabilize the antiparallel conformation. On comparison with binding constants, the results showed that the K_b values for $HTelo_8$ in KCl solution were nearly 10 to 15 times greater than the DNA solutions in antiparallel and no salt conditions. Each phase of the folding of G-quadruplex conformation is favoured by K^+ coordination because it reduces electrostatic repulsions. Since Na^+ residing in the center of the tetrads holds the guanines more tightly than K^+ which reduces the reactivity of the guanines not allowing to the investigated compound to interact with lateral loop. Moreover, the shorter eight-repeat sequence ($HTelo_8$) also exhibits a clear cation-dependent folding topology rather than higher-repeat one ($HTelo_{20}$). In addition, this is well correlated to our observation of modeling results that the guanine G10, despite being out of plane, seems well positioned to coordinate K^+ with its O6 resulted end stacking mode of binding interaction.

The right-handed double helix of CT DNA is defined by the positive band at 272 nm due to base stacking and the negative band at 242 nm due to right handed helicity. On interacting with the pure ligand dpyatriz and its Cu, Zn complexes, the right-handed helicity bands are affected little by decrease in intensity and the base stacking bands showed a slight shift (about 3 nm) with an increase in intensity (Fig. S8). The increase in intensity on the base stacking band on interaction with all three compounds can be attributed to the stacking interactions by the

Table 2 — Binding constant values K_b (M^{-1}) of dpyatriz, Cu-dpyatriz and Zn-dpyatriz complexes on interaction with telomere DNA

Compound	K_b (M^{-1}) values for $HTelo_8$			K_b (M^{-1}) values for $HTelo_{20}$		
	Parallel condition (100 mM KCl)	antiparallel condition (100 mM NaCl)	No salt condition	Parallel condition (100 mM KCl)	antiparallel condition (100 mM NaCl)	No salt condition
dpyatriz	4.2×10^7	3.16×10^5	1.5×10^6	4.3×10^5	7.0×10^5	7.6×10^5
Cu- dpyatriz	3.6×10^7	1.9×10^5	9.6×10^5	4.97×10^5	7.01×10^5	4.1×10^5
Zn- dpyatriz	9.3×10^6	4.6×10^5	1.2×10^6	4.7×10^5	6.8×10^5	9.2×10^5

compounds with the DNA bases[61]. The thermal denaturation experiments clearly demonstrated the strong binding of the compounds under no salt conditions, with ΔT_m values of 22, 27 and 35°C for dpyatriz, Zn-dpyatriz and Cu-dpyatriz, respectively[62].

According to these findings, the compounds intercalates to G-quadruplex and CT-DNA via π –π stacking on one or two different types of dependent binding sites. The high affinity site appears to undergo intercalation first, then the low affinity site. The number of binding sites for both types of sites is the same, with n = 6 for G-quadruplex and 9.3 x 10^5 for CT-DNA. According to these numbers, the G-quadruplex molecule has one binding site for every two base pairs while the CT-DNA molecule has two to three binding sites for every base pair. According to the binding constants, compounds had a similar or 10–12 higher affinity for G–quadruplex than CT–DNA. The increased hydrophobicity of the grooves in CT-DNA compared to those between the G-G-quartets quadruplex's may be the cause of compound's similar or lesser affinity for CT-DNA.

Fluorescent intercalator displacement (FID) assay

The binding affinity of the compounds under study towards G-quadruplex conformation of DNA was evaluated using a displacement assay. The compound thiazole orange intercalates with high affinity to G-quadruplex/double stranded stabilized DNA and emits on intercalation between the base pairs. Compounds are treated with G-quadruplex DNA which is already pre-treated with thiazole orange and the displacement of thiazole orange by the compounds under study would lead to then quenching of the thiazole orange emission induced due to intercalation on G-quadruplex/double stranded DNA[63,64]. The thiazole orange dye is also highly selective towards G-quadruplex over duplex DNA in comparison to ethidium bromide[65]. The assay is based on the decrease in fluorescence that follows when a ligand displaces the DNA intercalator thiazole orange from a DNA structure. Thiazole orange is excited at 510 nm and on intercalation it emits at 510 to 700 nm. The FID assay is done for $HTelo_{20}$ human telomeric DNA sequence stabilized in parallel (10 mM phosphate buffer, 100 mM KCl) and antiparallel (10 mM phosphate buffer, 100 mM NaCl) conditions. The dpyatriz, Cu-dpyatriz and Zn-dpyatriz compounds were then treated with G-quadruplex DNA which was already pre-treated with thiazole orange. When the pure ligand dpyatriz, Cu-dpyatriz and Zn-dpyatriz were added to the thiazole orange treated $HTelo_{20}$ under parallel conformation, the emission was fairly quenched by the free ligand dpyatriz. The emission of Cu-dpyatriz and Zn-dpyatriz were highly quenched (Fig. 4). The strong decrease of the fluorescence of the TO revealed the Cu and Zn complexes had higher affinity to G-quadruplex DNA and were binding strongly to the parallel conformation and TO was removed away from the G-quadruplex folding.

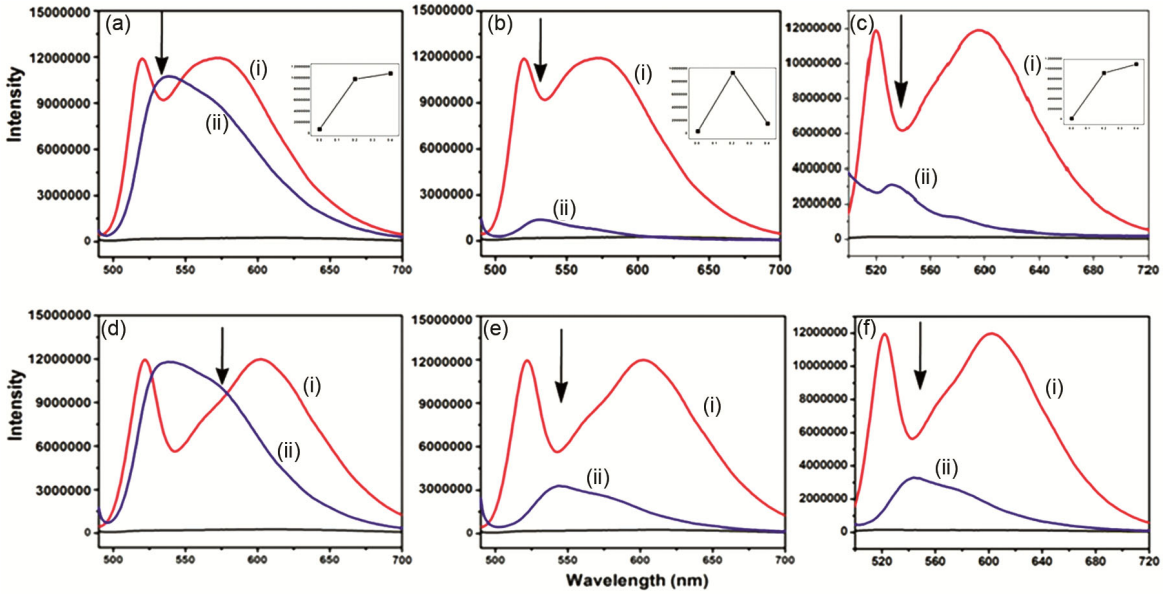

Fig. 4 — Emission spectra of TO in the presence of $HTelo_{20}$ stabilized under parallel G-quadruplex conformation before (i) and after treatment (ii) with dpyatriz (a), Cu-dpyatriz (b) and Zn- dpyatriz (c); Emission spectra of TO in the presence of $HTelo_{20}$ stabilized under antiparallel G-quadruplex conformation before (i) and after treatment (ii) with dpyatriz (d), Cu-dpyatriz (e) and Zn-dpyatriz (f)

The Cu-dpyatriz and Zn-dpyatriz showed TO emission quenching as observed for the parallel conformation, under the treatment of antiparallel conditions also. The pure ligand showed little emission intensity decrease under antiparallel G-quadruplex conditions. These results suggest the strong and effective binding of the compounds to the telomere DNA displacing the TO through an intercalative way (Fig. 4).

MOE molecular docking studies

The parallel, antiparallel and hybrid G-quadruplex forms of DNA were obtained from PDB for molecular docking experiments. The ligand and its Cu and Zn complexes were docked as described in the experimental. The major interactions, bond distances and energy of binding were presented in Table 3. 1KF1 from PDB was chosen for parallel G-quadruplex DNA, and converted to MOE file. The cations present in the central channel of 1KF1 were removed and energy minimized to leave the empty binding sites[66]. The ligand dpyatriz, Cu-dpyatriz and Zn-dpyatriz compounds were docked with 1KF1 and the binding modes were investigated. The ligand dpyatriz interacted in an end stacking mode on top of the G-quadruplex structure with strong interaction with G4, G10, G22 guanines (Fig. 5). The triazine and the pyridine ring of the dpyatriz ligand were involved in strong π-π and π-H interactions through end stacking mode with the G16 guanine base of DNA. The ligand showed weaker interactions with T17

Table 3 — Major interactions of dpyatriz, Cu-dpyatriz and Zn-dpyatriz with G-quadruplex DNA

Receptor	Compound	Ligand / complex atom in interaction	Receptor			Interaction	Distance (Å)	E (kcal/mol)
Parallel G quadruplex DNA (PDB ID: 1KF1)	dpyatriz	C 43	6-ring	DG	16	H-pi	4.42	-0.7
		6-ring	C2'	DG	16	pi-H	4.74	-0.9
	Cu-dpyatriz	N 56	OP1	DG	14	H-donor	3.18	-2.1
	Zn-dpyatriz	6-ring	6-ring	DG	8	pi-pi	3.90	-0.1
Anti parallel G quadruplex DNA (PDB ID: 2MCO)	dpyatriz	6-ring	C4'	DT	12	pi-H	4.00	-1.1
		C 49	5-ring	DA	13	H-pi	4.66	-0.7
		N 51	C1'	DT	12	H-acceptor	3.50	-0.7
	Cu-dpyatriz	N 34	OP2	DT	11	H-donor	3.05	-3.9
		Cu 76	OP2	DG	10	Metal	2.54	-1.2
		N 16	O4'	DT	12	H-donor	2.95	-3.0
	Zn-dpyatriz	Zn 79	OP2	DT	11	Metal	2.00	-3.0
		N 16	6-ring	DT	12	H-pi	4.63	-0.7
Hybrid -2 form of G quadruplex DNA (PDB ID: 6CCW)	dpyatriz	C 35	6-ring	DT	2	H-pi	3.36	-0.5
		C 41	6-ring	DG	12	H-pi	4.29	-0.6
	Cu-dpyatriz	Cl 81	O6	DG	16	H-donor	3.18	-2.5
		Cu 80	OP1	DG	6	Metal	2.65	-1.0
		N 36	6-ring	DT	13	H-pi	4.00	-3.1
		N 74	OP2	DT	14	H-donor	2.81	-11.6
	Zn-dpyatriz	Zn 76	OP1	DG	12	Metal	2.02	-2.3

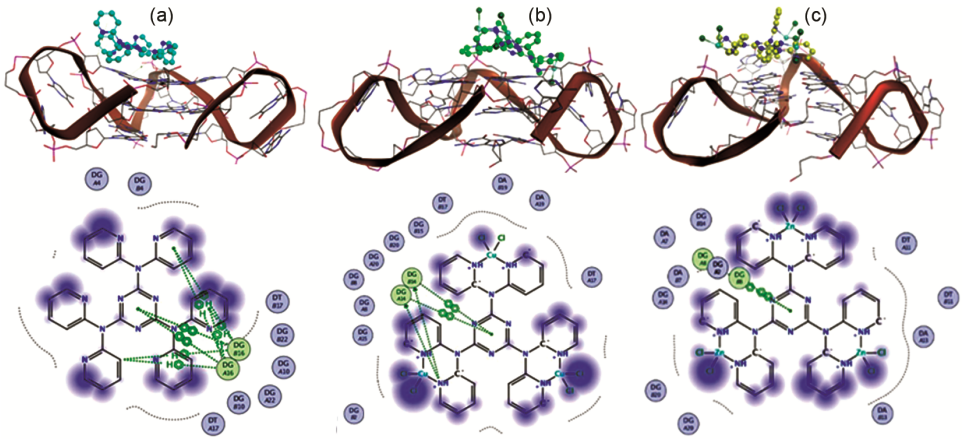

Fig. 5 — Docking pictures of parallel G-quadruplex strand with (a) dpyatriz, (b) Cu-dpyatriz, (c) Zn-dpyatriz and their interaction maps

thymine, G4, G10, and G22 guanines also. The Cu-dpyatriz interacted with the G14 guanine primarily in an end stacking mode. The G14 guanine was interacted highly with both the triazine and pyridine N part of the Cu-dpyatriz through π-π interactions. Secondary interactions were observed between the G2, G8, G15, G20, T17 and A19 bases of DNA and the Cu complex. The G8 guanine base of DNA was highly interacted with the Zn-dpyatriz through π-π interactions. The T11, A7, A13, G2, G14 and G20 bases showed secondary interactions with Zn-dpyatriz. Thus, the ligand dpyatriz, Cu-dpyatriz and Zn-dpyatriz compounds showed an end stacking mode of binding interaction with the parallel G quadruplex DNA.

For antiparallel DNA a NMR solution structure derived PDB file, 2MCO – the basket type antiparallel G-quadruplex structure was chosen for docking experiments[67]. The cations present in the central channel were again removed, energy minimized and then docked with dpyatriz, Cu-dpyatriz and Zn-dpyatriz. All the three compounds showed an intercalative mode of binding between the basket part of the antiparallel strand and the G-tetrad as binding result (Fig. 6). Strong π-π interactions were observed between G10, G14 and G22 guanine bases and the triazine, pyridine ring of the dpyatriz ligand. G2, G21 and T11 bases involved secondary interactions with the ligand. In Cu-dpyatriz, pyridine ring involved H-donor interactions with the G10, G14, G22 and T11 bases. Secondary interactions were involved with G2, G9, G14, G21 and T12 bases. Like Cu complex the Zn-dpyatriz, pyridine ring involved H-donor interactions with the T12 base. Prominently the Zn metal of Zn-dpyatriz complex involved in interaction with T11 base. Secondary interactions were also observed with G9, G10, G14, G22 and A13 bases with Zn complex. All the three compounds, the intercalative mode of interaction was observed with added interactions as described in Fig. 6. These extensive interactions might be the primary reason for these compounds to induce and stabilize the antiparallel G-quadruplex conditions.

Another NMR derived hybrid structure of telomere DNA (6CCW)[68] was also docked with the dpyatriz, Cu-dpyatriz and Zn-dpyatriz under the conditions as described above. Similar to the antiparallel G-quadruplex binding mode, intercalation mode of interaction was the primary binding modes for dpyatriz and Cu-dpyatriz. But the Zn-dpyatriz showed an end staking mode of interaction. Strong π-π interactions were observed with T2, T13 and G12 bases with pyridine ring of the dpyatriz. Secondary interactions were also observed between G4, G5, G6, G16, A3 and A15 bases and the ligand (Fig. 7). The total ligand intercalated between the G-quartets and

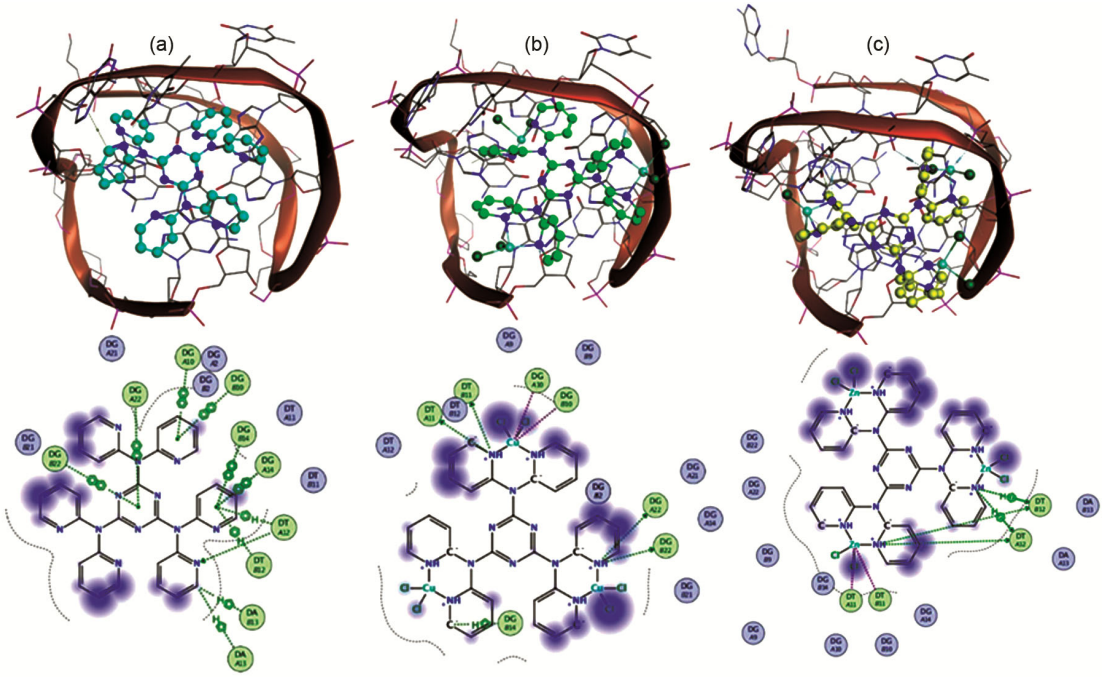

Fig. 6 — Docking pictures of antiparallel G-quadruplex strand with (a) dpyatriz, (b) Cu-dpyatriz, (c) Zn-dpyatriz and their interaction maps

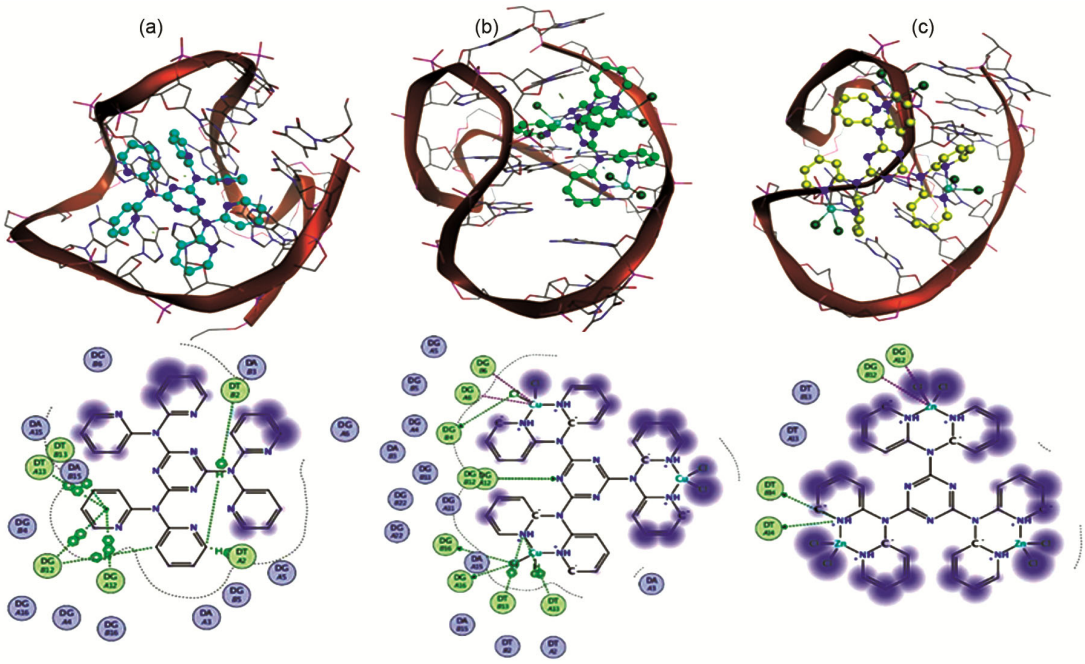

Fig. 7 — Docking pictures of hybrid G-quadruplex strand with (a) dpyatriz, (b) Cu-dpyatriz, (c) Zn-dpyatriz and their interaction maps

extended their binding, thus stabilizing the hybrid G-quadruplex conformation. On interaction with Cu-dpyatriz, H donor acceptor interactions were observed between chlorine, pyridine nitrogen of the ligand and G4, G12, G16 bases. The Cu metal of the Cu-dpyatriz also interacted with G6 guanine base. The H-π interaction was also observed between T13 base and Cu complex. Secondary interactions were observed between G4, G5, G11, G22, A3, A15 and T2 bases and Cu-dpyatriz. On interaction of Zn-dpyatriz with hybrid DNA, The Zn metal of the Zn-dpyatriz was interacted with G12 guanine base. The pyridine nitrogen of Zn-dpyatriz was involved in interaction with T14 base of the DNA. Secondary interactions were found between T13 base and with the Zn-dpyatriz complex. The Zn-dpyatriz was intercalated by end stacking binding mode shown in Fig. 7. Interaction report for parallel, antiparallel and hybrid DNA docking with all the three compounds are given in Tables S2-S10 in Supplementary Information.

Antitelomerase activity

The TRAP assay was done with reference to the previously published procedures[69]. The preliminary experiments towards antitelomerase activity showed inhibition of telomerase enzyme with IC_{50} values in 5-10 μM concentrations for the pure ligand and Cu, Zn complexes[70]. The IC_{50} values were presented in Table 4 and the procedure was described in

Table 4 — IC_{50} values of the compounds for their antitelomerase activity done through TRAP assay

Compound	IC_{50} value (μM)
dpyatriz	10
Cu-dpyatriz	5
Zn-dpyatriz	6

IC_{50} - 50% inhibitory concentration of telomerase activity

experimental. The concept of the experiment is the effective and stable induction of G-quadruplex forms especially from the intramolecular telomere sequence would then make the sequence unavailable for the telomerase enzyme to elongate it for the cell survival. Compounds showing weak or moderate binding to the G-quadruplex do not result in antitelomerase activity. Our compounds in the tested range (from 1 μM to 250 μM), do not show any elongation products except the control revealing the high induction of the G-quadruplex conformations on the telomere sequence. The intercalative mode of binding and further extended interactions by the multidendate ligand (dpyatriz) and with the coordinated metal ions in their Cu-dpyatriz and Zn-dpyatriz compounds rendered the stable G-quadruplex folding with biological significance and resulted in prominent antitelomerase activity.

Anticancer activity

The compounds dpyatriz, Cu-dpyatriz and Zn-dpyatriz were tested for anticancer activity against

Table 5 — IC_{50} values (in nM) of the compounds for their anticancer activity done through MTT assay on different cancer cell lines

Compounds	MCF7	M19-MEL	EVSA-T	A2780
dpyatriz	80	92	78	69
Cu-dpyatriz	50	62	56	72
Zn-dpyatriz	58	69	70	77

IC_{50} - 50% inhibitory concentration of cell growth

MCF7 (breast cancer cell line), M-19 MEL (human melanoma cancer cell line), EVSA-T (harmone independent human breast cancer cell line) and A2780 (ovarian carcinoma cell line). All the three compounds were very active with their IC_{50} values ranging in nanomolar concentrations (Table 5). The compounds stabilize the antiparallel G-quadruplex conformation, even under no salt conditions. The strong interaction of these compounds with telomere DNA towards G-quadruplex folding and stabilization may result in the interruption of the telomerase enzyme action and can be very effective as seen with the anticancer activities.

Conclusion

The dpyatriz, Cu-dpyatriz and Zn-dpyatriz compounds induce and stabilize antiparallel G-quadruplex conformations in both short and long range human telomeric sequences, both in the presence and absence of alkali ions. The CD studies reveal the strong stabilization of the G-quadruplex forms on interaction with the above compounds. The FID assays also reveal the strong binding of the compounds with the G-quadruplex stabilized form by displacing the bound thiazole orange. Molecular docking studies on the G-quadruplex stabilized sequence models with the compounds under induced fit conditions revealed the intercalative mode of interaction of the compounds as the most preferred one. The formed G-quadruplexes were thermodynamically stable and irreversible, thus resulting in efficient antitelomerase and anticancer activity *in-vitro*.

Acknowledgement

Prof. Raghavan, MBU, IISc, Bangalore thanked for CD facility. DST-WOS-A (SR/WOS-A/CS-75/2016), India is acknowledged for financial support.

Supplementary Information

Supplementary information is available in the website http://nopr.niscpr.res.in/handle/123456789/58776.

References

1 Jafri M A, Ansari S A, Alqahtani M H & Shay J W, *Genome Med*, 8 (2016) 69.
2 Meyerson M, *J Clin Oncol*, 18 (2000) 2626.
3 Meyerson M, Counter C M, Ng Eaton E, Ellisen L W, Steiner P, Dickinson Caddle S, Ziaugra L, Beijersbergen R L, Davidoff M J, Liu Q, Bacchetti S, Haber D A & Weinberg R A, *Cell*, 90 (1997) 785.
4 Gyawali P, Keshav G C, Ma Y, Abeysirigunawardena S, Nagasawa K & Balci H, *Molecules*, 24 (2019) 1.
5 Chen M, Song G, Wang C, Hu D, Ren J & Qu X, *Biophys J*, 97 (2009) 2014.
6 Luedtke N W, *CHIMIA Inter J Chem*, 63 (2009) 134.
7 Awadasseid A, Ma X, Wu Y & Zhang W, *Biomed Pharmacother*, 139 (2021) 111550.
8 Zhou B S & Elledge S J, *Nature*, 408 (2000) 433.
9 Zambre V P, Murumkar P R, Giridhar R & Yadav M R, *J Chem Inf Model*, 49 (2009) 1298.
10 Si M K, Pramanik S K & Ganguly B, *Int J Biol Macromol*, 124 (2019) 1177.
11 Percivalle C, Sissi C, Greco M L, Musetti C, Mariani A, Artese A, Costa G, Perrore M L, Alcaroc S & Freccero M, *Org Biomol Chem*, 12 (2014) 3744.
12 Tikhomirov A S, Tsvetkov V B, Kaluzhny D N, Volodina Y L, Zatonsky G V, Schols D, & Shchekotikhin A E, *Eur J Med Chem*, 159 (2018) 59.
13 Zhang L M, Cui Y X, Zhu L N, Chu J Q & Kong D M, *Nucleic Acids Res*, 47 (2019) 2727.
14 Han J H, Cho H Y, Kim D Y, Jang Y J, Lee Y A & Kim S K, *J Mol Struct*, 1215 (2020) 128264.
15 Franceschin M, Lombardo C M, Pascucci E, D'Ambrosio D, Micheli E, Bianco A, Ortaggi G & Savino M, *Bioorganic Med Chem*, 16 (2008) 2292.
16 Mulhollandand K & Wu C, *J Chem Inf Model*, 56 (2016) 2093.
17 Doria F, Pirota V, Petenzi M, Teulade-Fichou M P, Verga D & Freccero M, *Molecules*, 23 (2018) 2162.
18 Riou J F, Guittat L, Mailliet P, Laoui A, Renou E, Petitgenet O, Megnin-Chanet F, Helene C & Mergny J L, *Proc Natl Acad Sci U S A*, 99 (2002) 2672.
19 Ranjan N, Andreasen K F, Arora Y, Xue L & Arya D P, *Front Chem*, 8 (2020) 60.
20 Wu Q, Song Y, Liu R, Wang R, Mei W, Chen W, Yang H & Wang X, *Bioorg Chem*, 102 (2020) 104074.
21 Singh A K, Yadav M, Pandey R, Kumar P & Pandey D S, *J Organomet Chem*, 695 (2010) 1932.
22 Pang J, Marcotte E J P, Seward C, Brown R S & Wang S, *Angew Chemie - Int Ed*, 40 (2001) 4042.
23 Liu Q D, Jia W L, Wu G & Wang S, *Organometallics*, 22 (2003) 3781.
24 Yang W, Chen L & Wang S, *Inorg Chem*, 40 (2001) 507.
25 Pang J, Tao Y, Freiberg S, Yang X P, D'Iorio M & Wang S, *J Mater Chem*, 12 (2002) 206.
26 Gamez P, De Hoog P, Lutz M, Spek A L & Reedijk J, *Inorganica Chim Acta*, 351 (2003) 319.
27 Hajra T, Bera J K & Chandrasekhar V, *Inorganica Chim Acta*, 372 (2011) 53.

28 Quesada M, De La Pena-O'Shea V A, Aromi G, Geremia S, Massera C, Roubeau O, Gamez P & Reedijk J, *Adv Mater*, 19 (2007) 1397.

29 Quesada M, De Hoog P, Gamez P, Roubeau O, Aromi G, Donnadieu B, Massera C, Lutz M, Spek A L & Reedijk J, *Eur J Inorg Chem*, 2006 (2006) 1353.

30 Casellas H, Roubeau O, Teat S J, Masciocchi N, Galli S, Sironi A, Gamez P & Reedijk J, *Inorg Chem*, 46 (2007) 4583.

31 Asman P W, *Inorganica Chim Acta*, 469 (2018) 341.

32 Gamez P, Hoog P De, Lutz M, Driessen W L, Spek A L & Reedijk J, *Polyhedron*, 22 (2003) 205.

33 Seward C, Pang J & Wang S, *Eur J Inorg Chem*, 2000 (2002) 1390.

34 Demeshko S, Leibeling G, Dechert S & Meyer F, *Dalt Trans*, (2004) 3782. (https://doi.org/10.1039/B407598F)

35 Chen J, Wang X, Shao Y, Zhu J, Zhu Y, Li Y, Xu Q & Guo Z, *Inorg Chem*, 46 (2007) 3306.

36 Wong E, Li J, Seward C & Wang S, *Dalt Trans*, (2009) 1776, (https://doi.org/10.1039/B814393E).

37 Seward C, Jia W L, Wang R Y & Wang S, *Inorg Chem*, 43 (2004) 978.

38 De Hoog P, Gamez P, Driessen W L & Reedijk J, *Tetrahedron Lett*, 43 (2002) 6783.

39 Maheswari P U, Modec B, Pevec A, Kozlevcar B, Massera C, Gamez P & Reedijk J, *Inorg Chem*, 45 (2006) 6637.

40 Wolfe A, Shimer G H & Meehan T, *Biochemistry*, 26 (1987) 6392.

41 Bhattacharjee A J, Ahluwalia K, Taylor S, Jin O, Nicoludis J M, Buscaglia R, Chaires J B, Kornfilt D J P, Marquardt D G S & Yatsunyk L A, *Biochimie*, 93 (2011) 1297.

42 Alley M C, Scudiero D A , Monks A, Hursey M L, Czerwinski M J, Fine D L, Abbott B J, Mayo J G, Shoemaker R H & Boyd M R, Cancer Res, 48 (1988) 589.

43 Sun L, Jin H, Zhao X, Liu Z, Guan Y, Yang Z, Zhang L & Zhang L, *Chem Med Chem*, 9 (2014) 993.

44 Dhamodharan V, Harikrishna S, Jagadeeswaran C, Halder K & Pradeepkumar P I, *J Org Chem*, 77 (2012) 229.

45 Nagatoishi S, Tanaka Y & Tsumoto K, *Biochem Biophys Res Commun*, 352 (2007) 812.

46 Toro M del, Gargallo R, Eritja R & Jaumot J, *Anal Biochem*, 379 (2008) 8.

47 Goncalves D P N, Rodriguez R, Balasubramanian S & Sanders J K M, *Chem Commun*, 2 (2006) 4685.

48 Zhang W J, Ou T M, Lu Y J, Huang Y Y, Wu W B, Huang Z S, Zhou J L, Wong K Y & Gu L Q, *Bioorganic Med Chem*, 15 (2007) 5493.

49 Vorlickova M, Chladkova J, Kejnovska I, Fialova M & Kypr J, *Nucleic Acids Res*, 33 (2005) 5851.

50 Rujan I N, Meleney J C & Bolton P H, *Nucleic Acids Res*, 33 (2005) 2022.

51 Chang C C, Chien C W, Lin Y H, Kang C C & Chang T C, *Nucleic Acids Res*, 35 (2007) 2846.

52 Xu Y, Noguchi Y & Sugiyama H, *Bioorganic Med Chem*, 14 (2006) 5584.

53 Matsugami A, Xu Y, Noguchi Y, Sugiyama H & Katahira M, *FEBS J*, 274 (2007) 3545.

54 He Y, Neumann R D & Panyutin I G, *Nucleic Acids Res*, 32 (2004) 5359.

55 Kovacic M, Podbevsek P, Tateishi-Karimata H, Takahashi S, Sugimoto N & Plavec J, *Nucleic Acids Res*, 48 (2020) 3975.

56 Yang S, Xiang J, Yang Q, Zhou Q, Zhang X, Li Q, Li Q, Tang Y & Xu G, *Fitoterapia*, 81 (2010) 1026.

57 Roshatiara S, Sahudin M A, Hassan N H & Karim N H A, *Malaysian J Anal Sci*, 21 (2017) 544.

58 Terenzi A, Bonsignore R, Spinello A, Gentile C, Martorana A, Ducani C, Hogberg B, Almerico A M, Lauria A & Barone G, *RSC Adv*, 4 (2014) 33245.

59 Fu B, Zhang D, Weng X, Zhang M, Heng M, Yuzhi M & Zhou X, *Chem - A Eur J*, 14 (2008) 9431.

60 Xu L, Liao G L, Chen X, Zhao C Y, Chao H & Ji L N, *Inorg Chem Commun*, 13 (2010) 1050.

61 Bordbar M, Tavoosi F, Yeganeh-Faal A & Zebarjadian M H, *J Mol Struct*, 1152 (2018) 128.

62 Marchand A, Rosu F, Zenobi R & Gabelica V, *J Am Chem Soc*, 140 (2018) 12553.

63 Largy E, Hamon F & Teulade-Fichou M P, *Anal Bioanal Chem*, 400 (2011) 3419.

64 Monchaud D, Allain C & Teulade-Fichou M P, *Bioorganic Med Chem Lett*, 16 (2006) 4842.

65 Lubitz I, Zikich D & Kotlyar A, *Biochemistry*, 49 (2010) 3567.

66 Parkinson G N, Lee M P H & Neidle S, *Nature*, 417 (2002) 876.

67 Wilson T, Costa P J, Felix V, Williamson M P & Thomas J A, *J Med Chem*, 56 (2013) 8674.

68 Lin C, Wu G, Wang K, Onel B, Sakai S, Shao Y & Yang D, *Angew Chemie - Int Ed*, 57 (2018) 10888.

69 Mender I & Shay J W, *Bio-Protocol*, 5 (2016) 1657.

70 Shin-ya K, Wierzba K, Matsuo K, Ohtani T, Yamada Y, Furihata K, Hayakawa Y & Seto H, *J Am Chem Soc*, 123 (2001) 1262.